The missing massive satellites of the Milky Way

Jie Wang,[1] Carlos S. Frenk,[1]⋆ Julio F. Navarro,[2] Liang Gao[3] and Till Sawala[1]

[1]*Department of Physics, Institute for Computational Cosmology, University of Durham, South Road, Durham DH1 3LE*
[2]*Department of Physics and Astronomy, University of Victoria, PO Box 3055 STN CSC, Victoria, BC, V8W 3P6, Canada*
[3]*National Astronomical Observatories, Chinese Academy of Sciences, Beijing 100012, China*

ABSTRACT

Recent studies suggest that only three of the 12 brightest satellites of the Milky Way (MW) inhabit dark matter haloes with maximum circular velocity, $V_{\rm max}$, exceeding ∼30 km s^{-1}. This is in apparent contradiction with the Λ cold dark matter (CDM) simulations of the Aquarius Project, which suggest that MW-sized haloes should have at least eight subhaloes with $V_{\rm max} > 30$ km s^{-1}. The absence of luminous satellites in such massive subhaloes is thus puzzling and may present a challenge to the ΛCDM paradigm. We note, however, that the number of massive subhaloes depends sensitively on the (poorly known) virial mass of the MW, and that their scarcity makes estimates of their abundance from a small simulation set like Aquarius uncertain. We use the Millennium Simulation series and the invariance of the scaled subhalo velocity function (i.e. the number of subhaloes as a function of ν, the ratio of the subhalo $V_{\rm max}$ to the host halo virial velocity, V_{200}) to secure improved estimates of the abundance of rare massive subsystems. In the range $0.1 < \nu < 0.5$, $N_{\rm sub}(>\nu)$ is approximately Poisson distributed about an average given by $\langle N_{\rm sub} \rangle = 10.2\,(\nu/0.15)^{-3.11}$. This is slightly lower than that in Aquarius haloes, but consistent with recent results from the Phoenix Project. The probability that a ΛCDM halo has three or fewer subhaloes with $V_{\rm max}$ above some threshold value, $V_{\rm th}$, is then straightforward to compute. It decreases steeply both with decreasing $V_{\rm th}$ and with increasing halo mass. For $V_{\rm th} = 30$ km s^{-1}, ∼40 per cent of $M_{\rm halo} = 10^{12}$ M$_\odot$ haloes pass the test; fewer than ∼5 per cent do so for $M_{\rm halo} \gtrsim 2 \times 10^{12}$ M$_\odot$ and the probability effectively vanishes for $M_{\rm halo} \gtrsim 3 \times 10^{12}$ M$_\odot$. Rather than a failure of ΛCDM, the absence of massive subhaloes might simply indicate that the MW is less massive than is commonly thought.

Key words: Galaxy: abundances – Galaxy: halo – dark matter.

1 INTRODUCTION

The striking difference between the relatively flat faint-end slope of the galaxy stellar mass function and the much steeper cold dark matter (CDM) halo mass function is usually reconciled by assuming that the efficiency of galaxy formation drops sharply with decreasing halo mass (see e.g. White & Frenk 1991). Semi-analytic models of galaxy formation have used this result to explain the relatively small number of luminous satellites in the Milky Way (MW) halo, where ΛCDM simulations predict the existence of thousands of subhaloes massive enough, in principle, to host dwarf galaxies. In these models, the small number of MW satellites reflects the relatively small number of subhaloes massive enough to host luminous galaxies (see e.g. Kauffmann, White & Guiderdoni 1993; Bullock, Kravtsov & Weinberg 2000; Benson et al. 2002; Somerville 2002;

Cooper et al. 2010; Li, De Lucia & Helmi 2010; Macciò et al. 2010; Font et al. 2011; Guo et al. 2011).

This is a model prediction that can be readily tested observationally, given the availability of radial velocity measurements for hundreds of stars in the dwarf spheroidal satellites of the MW. Combined with photometric data, radial velocities tightly constrain the total mass enclosed within the luminous radius of these satellites (Walker et al. 2009; Wolf et al. 2010). The latter correlates strongly with the total dark mass of the dwarf, which is usually expressed in terms of its maximum circular velocity $V_{\rm max}$, a quantity less affected than mass by tidal stripping (Peñarrubia, Navarro & McConnachie 2008b).

Kinematical analyses of the MW dwarf spheroidals have been attempted by several authors in recent years, with broad consensus on the results, at least for the best-studied nine brightest dwarf spheroidal MW companions: Draco, Ursa Minor, Fornax, Sculptor, Carina, Leo I, Leo II, Canis Venatici I and Sextans (see e.g. Peñarrubia, McConnachie & Navarro 2008a; Strigari et al. 2008;

Łokas 2009; Walker et al. 2009; Strigari, Frenk & White 2010; Wolf et al. 2010). These studies suggest that some of these galaxies may inhabit haloes with V_{max} as low as 12 km s^{-1} and agree that all[1] appear to inhabit haloes with values of V_{max} below a low threshold, $V_{th} \sim 30$ km s^{-1}. Only three dwarf irregular satellites – the Magellanic Clouds and the Sagittarius dwarf – may, in principle, inhabit haloes exceeding this threshold.

The most straightforward interpretation of this result is that massive subhaloes in the MW are rare. However, as argued recently by Boylan-Kolchin, Bullock & Kaplinghat (2011, 2012), this is at odds with the results of the Aquarius Project, a series of N-body simulations of six different haloes of virial[2] masses in the range $0.8 < M_{200}/10^{12}\,\mathrm{M}_\odot < 1.8$. Boylan-Kolchin et al. (2011) noted that the largest subhaloes in these simulations are significantly denser than that inferred for the haloes that host the brightest dwarf spheroidals in the MW.

As discussed by Parry et al. (2012) and Boylan-Kolchin et al. (2012), the discrepancy can be traced to the fact that the largest Aquarius subhaloes are significantly more massive or, equivalently, have too large a value of V_{max} to be compatible with the measured kinematics of the brightest dwarf spheroidals. Specifically, the Aquarius haloes have, on average, approximately eight subhaloes with $V_{max} > 30$ km s^{-1} within the virial radius, larger than the V_{max} of the brightest dwarf spheroidals, prompting questions like why these massive subhaloes fail to host luminous satellites in the MW. If this result holds, it may point to a failure of our basic understanding of how galaxies populate low-mass haloes or, more worryingly, of the ΛCDM paradigm itself.

Two issues may affect these conclusions. One is that the Aquarius Project simulation set contains only six haloes and, therefore, estimates of the abundance of rare massive subhaloes are subject to substantial uncertainty. The second point is that the number of massive subhaloes is expected to depend sensitively on the virial mass of the host halo, which is only known to be within a factor of 2–3 for the MW.

We address these issues here by using large numbers of well-resolved haloes identified in the Millennium Simulation series (Springel et al. 2005; Boylan-Kolchin et al. 2009). This is possible because, in agreement with earlier work, we find that the abundance of subhaloes, when scaled appropriately, is independent of halo mass (see e.g. Moore et al. 1999; Kravtsov et al. 2004; Springel et al. 2008). We use this to derive the improved estimates of the average number of massive subhaloes, as well as its statistical distribution. The probability that a halo has as a few massive subhaloes as the MW can then be evaluated both as a function of the host halo mass and/or the subhalo mass threshold.

This paper is organized as follows. Section 2 describes briefly the simulations we used in our analysis. We present our main results in Section 3 and end with a brief summary in Section 4.

2 SIMULATIONS

The two Millennium Simulations (MS; Springel et al. 2005 and MS-II; Boylan-Kolchin et al. 2009) provide the main data sets used in this study. Both are simulations of a flat *Wilkinson Microwave Anisotropy Probe* (*WMAP*)-1 ΛCDM cosmogony with the following parameters: $\Omega_M = 0.25$, $\Omega_b = 0.045$, $h = 0.73$, $n_s = 1$ and $\sigma_8 = 0.9$.

The MS run evolved a 500 Mpc h^{-1} box on a side, with 2160^3 particles of mass $m_p = 8.6 \times 10^8\,\mathrm{M}_\odot\,h^{-1}$. MS-II evolved the same total number of particles in a box 1/125 the volume of MS and had, therefore, 125 times better mass resolution ($m_p = 6.885 \times 10^6\,\mathrm{M}_\odot\,h^{-1}$). The nominal spatial resolution is given by the Plummer-equivalent gravitational softening, which is $\epsilon_P = 5$ and 1 kpc h^{-1} for the MS and MS-II runs, respectively.

We also use haloes from the Aquarius Project (Springel et al. 2008) and the Phoenix Project (Gao et al. 2012, level-2 resolution). These are the ultra-high-resolution simulations of six MW-sized haloes ($M_{200} \sim 10^{12}\,\mathrm{M}_\odot$) and nine cluster-sized haloes ($M_{200} \sim 10^{15}\,\mathrm{M}_\odot$), each resolved with a few hundred million particles within the virial radius.

The normalization of the power spectrum adopted in these simulations is slightly higher than that favoured by the latest *WMAP* data set (*WMAP*7; Komatsu et al. 2011), but this is expected to affect the abundance of haloes of given virial mass rather than the mass function of subhaloes, which is the main focus of our study. We have verified this explicitly by analysing a 1620^3-particle simulation of a 70.4 Mpc h^{-1} box that adopts the *WMAP*7 cosmological parameters (see Fig. 1). The particle mass in this run is $6.20 \times 10^6\,\mathrm{M}_\odot\,h^{-1}$ and gravitational interactions were softened with $\epsilon_P = 1$ kpc h^{-1}.

Haloes and subhaloes are identified in all simulations by SUBFIND (Springel, Yoshida & White 2001), a recursive algorithm that identifies self-bound structures and substructures in N-body simulations.

3 RESULTS

We first investigate the scale invariance and other statistical properties of the distribution of subhalo V_{max} and then apply our results to subhaloes in the MW.

3.1 Subhalo V_{max} distribution

Fig. 1 shows, as a function of the host halo virial mass, the total number[3] of subhaloes with maximum circular velocity, V_{max}, exceeding a specified velocity threshold, V_{th}. Results are shown for three different values of V_{th}. The average number of subhaloes in each halo mass bin is shown by symbols connected by solid (MS-II) or dashed (MS) lines. Individual level-2 Phoenix and Aquarius haloes are shown by crosses and open squares, respectively. *WMAP*7 results are shown by open triangles connected by a dotted line.

Fig. 1 illustrates that (i) the number of subhaloes depends roughly linearly on halo mass and increases strongly with decreasing velocity threshold, and that (ii) the slight change in cosmological parameters from *WMAP*1 to *WMAP*7 has a negligible effect on subhalo abundance.

Fig. 1 also shows that numerical resolution limits the halo mass and velocity threshold for which convergence in subhalo abundances is achieved. Indeed, there are fewer subhaloes in MS, the simulation with poorest mass resolution; so few with velocities less than ~100 km s^{-1} that the $V_{th} = 30$ and 60 km s^{-1} MS curves have been omitted for clarity. When haloes and subhaloes are resolved with enough particles; however, the results converge well. For

---

[1] One possible exception is Draco, where the data might allow a more massive halo.

[2] Unless otherwise noted, we define virial quantities as those corresponding to spheres that enclose a mean overdensity $\Delta = 200$ times the critical density for closure. M_{200}, for example, corresponds to the mass within the virial radius, r_{200}. When other values of Δ are assumed the subscript is adjusted accordingly.

[3] Unless otherwise noted, we identify subhaloes within the virial radius, r_{200}, of the host halo.
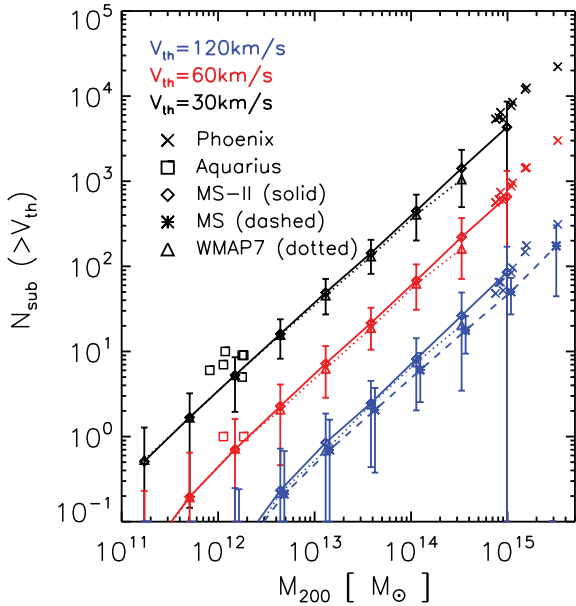
Figure 1. The number of subhaloes with $V_{\max} \geq V_{\mathrm{th}}$ as a function of the virial mass of their host haloes, M_{200}, in the Millennium Simulations (MS and MS-II), as well as in the level-2 runs of the Aquarius and Phoenix Projects. Subhaloes are identified within the virial radius, r_{200}, of their host systems. Different symbols correspond to each simulation, as labelled, and are coloured according to the value of the threshold, V_{th}. The error bars denote the rms plus Poisson error in each mass bin. Note the nearly linear dependence of the number of subhaloes on halo mass. Due to numerical resolution, a few subhaloes with velocities less than $\sim$100 km s^{-1} are found in the MS, so the $V_{\mathrm{th}} = 30$ and 60 km s^{-1} MS curves in this case are omitted for clarity. For massive, well-resolved haloes, the results are much less affected by numerical limitations and there is good agreement between MS and MS-II. Subhalo abundance is insensitive to small variations in the cosmological parameters. The triangles connected by a dotted line show results corresponding to a run that adopted the latest *WMAP*7 parameters (Komatsu et al. 2011); in contrast, the Millennium Simulations adopted parameters consistent with the first-year analysis of *WMAP* data.

$V_{\mathrm{th}} = 120$ km s^{-1}, MS, MS-II and *WMAP*7 haloes yield similar numbers of subhaloes over the whole halo mass range considered, despite the fact that, at given M_{200}, MS-II and *WMAP*7 haloes have $\sim$125 times more particles than their MS counterparts. Furthermore, the results for Phoenix and Aquarius are in good agreement with MS-II, even though haloes in MS-II have 700 times fewer particles than Aquarius and two times fewer than Phoenix, respectively.

We explore the requirements for numerical convergence in more detail in Fig. 2, where we plot, as a function of the total number of particles within the virial radius N_{200}, the average number of subhaloes with $V_{\max}$ exceeding a certain fraction of the host halo virial velocity: $N_{\mathrm{sub}}(>\nu)$, for $\nu = V_{\max}/V_{200} = 0.10, 0.15$ and 0.20. Results are shown for MS and MS-II haloes with dashed and solid curves, respectively.

This figure highlights two important points. One is that at given ν there is good agreement between all simulations provided that haloes are resolved with enough particles. The second is that, when the first condition is met, $N_{\mathrm{sub}}(>\nu)$ is independent of halo mass. (Recall that, at fixed N_{200}, MS haloes are 125 times more massive than their MS-II counterparts.) This agreement, together with the fact that the $N_{\mathrm{sub}}(>\nu)$ curves plateau at large values of N_{200}, implies that the *scaled* subhalo velocity function (i.e. the number of subhaloes as a function of $\nu = V_{\max}/V_{200}$) is invariant over many
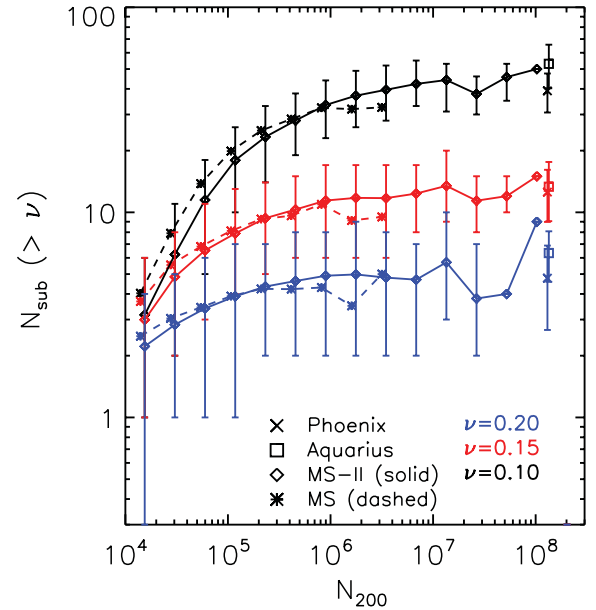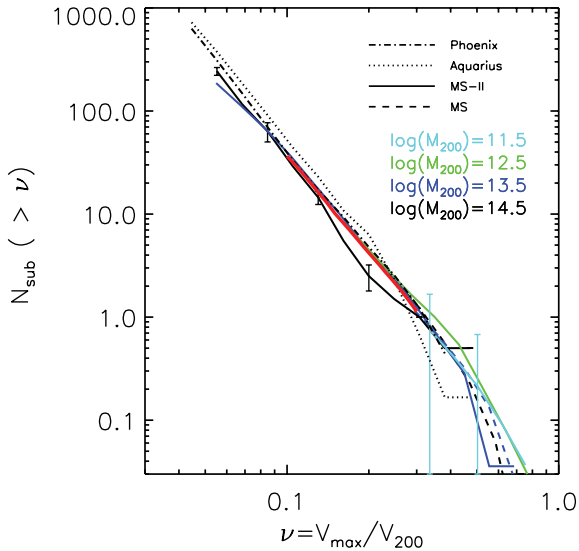

Figure 2. The number of subhaloes with maximum circular velocity exceeding a certain fraction, ν, of their host halo virial velocity as a function of N_{200}, the number of particles within the virial radius of the host. Curves for three values of $\nu = 0.1, 0.15$ and 0.2 are shown. The error bars for MS and MS-II indicate the 10 and 90 percentile in each bin, and are omitted when the bin contains a single halo. The excellent agreement between the results for MS and MS-II at given N_{200} reflects the halo mass invariance of the $N_{\mathrm{sub}}(>\nu)$ function; each particle is 125 times more massive in MS than in MS-II. Results converge for well-resolved haloes (i.e. those with large N_{200}). As expected, the smaller the ν the larger the minimum number of particles, $N_{200}^{\min}$, needed to obtain converged results.

decades in halo mass. Fig. 2 also makes it clear that numerical convergence requires that a halo be resolved with a total number of particles above some (ν-dependent) minimum number, $N_{200}^{\min}$ (listed in Table 1). The converged values agree well, within the statistical uncertainty, with the results for Phoenix and Aquarius haloes.

We show the invariance of subhalo abundance explicitly in Fig. 3, where $N_{\mathrm{sub}}(>\nu)$ is plotted for MS and MS-II haloes grouped in four bins of different halo masses. Only haloes satisfying the $N_{200} > N_{200}^{\min}$ constraint are used here. These results confirm earlier work (see e.g. Moore et al. 1999; Kravtsov et al. 2004; Zheng et al. 2005; Springel et al. 2008; Weinberg et al. 2008) and imply that we can combine all well-resolved haloes into one large sample to derive robust estimates of the statistical *distribution* of $N_{\mathrm{sub}}(>\nu)$.

This is shown in Fig. 4 for $\nu = 0.1, 0.15$ and 0.2, computed using all MS and MS-II haloes with $N_{200} > N_{200}^{\min}(\nu)$, as given in Table 1. In the top panel, which corresponds to subhaloes identified within r_{200}, the histograms show the $N_{\mathrm{sub}}(>\nu)$ distributions for the 614, 3070 and 6867 haloes that satisfy the minimum particle number constraint. The bottom panel shows subhalo numbers identified within a slightly larger radius, r_{100}, which is on average $\sim$30 per cent larger than r_{200}. (The mean and rms dispersion of the distributions of $N_{\mathrm{sub}}(>\nu)$ are listed in Table 1.) Note that the results obtained for MS and MS-II are in excellent agreement with those obtained for Phoenix haloes. Subhaloes in Aquarius are slightly overabundant, perhaps because of small biases in their assembly histories (Boylan-Kolchin et al. 2010), but still consistent with the MS and MS-II results given the large variance ($\sigma_{N_{\mathrm{sub}}}^2$) expected from the sample of only six Aquarius haloes. Note also that, as expected, the larger volume encompassed by r_{100} yields larger subhalo numbers than that

Figure 3. The scaled subhalo velocity function, i.e. the number of subhaloes with maximum circular velocity exceeding a certain fraction, $\nu = V_{max}/V_{200}$, of the host halo virial velocity. The dotted and dot–dashed curves show averages for the six Aquarius haloes and nine Phoenix haloes, respectively. The dashed and solid curves correspond to MS and MS-II. Four curves are shown for each, corresponding to averages over all haloes in the mass bins of width 0.1 dex centred at $\log_{10} M_{200}/M_{\odot} = 11.5, 12.5, 13.5$ and 14.5. The error bars (shown only for the lowest and highest mass bins) indicate the *rms* scatter in each bin. Only haloes satisfying the constraint $N_{200} > N_{200}^{min}(\nu)$ are used. All simulations are in good agreement when well-resolved haloes are considered. The scaled subhalo velocity function is thus nearly invariant with mass. See the text for further discussion.

found when identifying subhaloes only within r_{200}. For $r < r_{200}$, the average $N_{sub}(>\nu)$ is a steep function of ν, well approximated, in the range $0.1 < \nu < 0.5$, by

$$\langle N_{sub} \rangle (>\nu) = 10.2 \, (\nu/0.15)^{-3.11}. \tag{1}$$

Fig. 4 also shows that the distribution of $N_{sub}(>\nu)$ follows Poisson statistics closely; the solid curves are actually *not* fits, but just Poisson distributions with the same average as each of the histograms. Clearly, these provide a good description of the distribution of $N_{sub}(>\nu)$ at fixed ν. This conclusion is supported by earlier work (see e.g. Kravtsov et al. 2004; Boylan-Kolchin et al. 2010), as well as the data listed in Table 1: the average number of subhaloes is roughly similar to the variance, as expected from a Poisson process.

3.2 Massive satellites in the MW

We can use these results to address the MW missing massive satellites problem highlighted in Section 1. In particular, it is straightforward to compute the probability that a halo has X or fewer subhaloes with $V_{max} > 30 \, \mathrm{km \, s^{-1}}$ within its virial radius, once a virial mass (or, equivalently, a virial velocity, V_{200}) has been assumed for the MW. This is given by

$$f(\leq X) = \sum_{k=0}^{X} \frac{\lambda_{\nu}^{k}}{k!} e^{-\lambda_{\nu}}, \tag{2}$$

where $\lambda_{\nu} = \langle N_{sub} \rangle (>\nu)$ is given by equation (1).

The solid black curve in Fig. 5 shows $f(\leq 3)$ as a function of virial mass (upper tick marks on the abscissa) or virial velocity (lower tick marks). The probability is a steep function of the assumed halo mass: more than 40 per cent of $10^{12} \, M_{\odot}$ haloes pass this test, but only
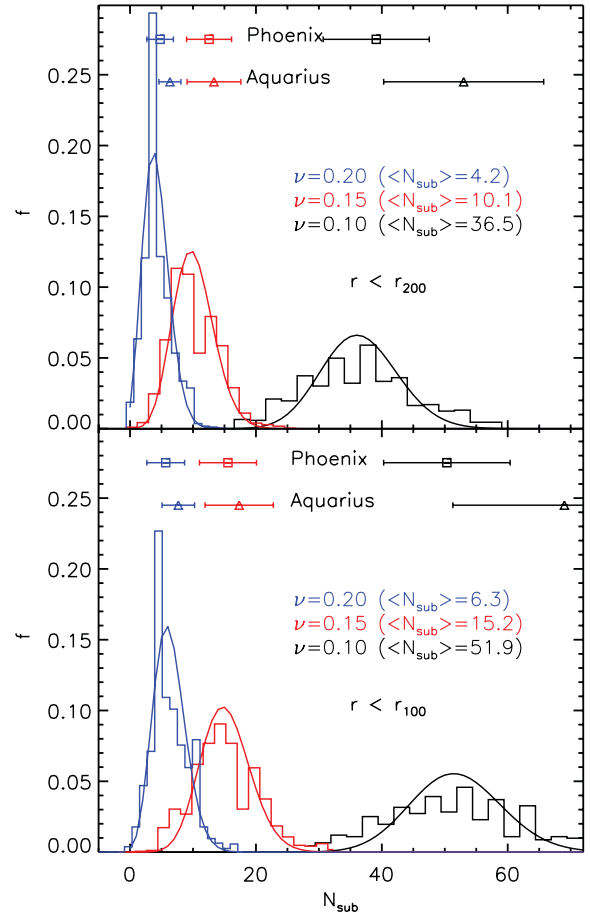

Figure 4. The distribution of $N_{sub}(>\nu)$ for $\nu = 0.1, 0.15$ and 0.2 computed for well-resolved MS and MS-II haloes, i.e. those with particle numbers exceeding $N_{200}^{min}(\nu)$ (as given in Table 1). The top panel refers to all subhaloes within the virial radius, r_{200}; the bottom panel refers to subhaloes within a radius roughly 30 per cent larger, r_{100}. The average and rms for Aquarius and Phoenix haloes are shown at the top of the plot. Note that subhaloes in Aquarius seem slightly overabundant relative to either Phoenix or the Millennium Simulations, but still well within the statistical uncertainty. The $N_{sub}(>\nu)$ distribution is well approximated by a Poisson distribution: the solid curves show Poisson distributions with the same averages as each histogram.

~5 per cent of $2 \times 10^{12} \, M_{\odot}$ systems do so. The probability becomes negligible for $M_{200} \gtrsim 3 \times 10^{12} \, M_{\odot}$. This suggests that the scarcity of massive subhaloes is best thought of as placing a strong upper limit on the virial mass of the MW, rather than as a failure of the ΛCDM scenario.

It is important to assess the sensitivity of this conclusion to the parameters assumed in this study. For example, should the velocity threshold be placed at $25 \, \mathrm{km \, s^{-1}}$, rather than at $30 \, \mathrm{km \, s^{-1}}$, as argued by Boylan-Kolchin et al. (2012), the upper limit on the mass of the MW would become even more restrictive. The results, however, could still be read from Fig. 5, after shifting the tick marks by $30/25 = 1.2$ in the velocity axis or by $1.2^3 = 1.73$ in the mass axis. Thus, for $V_{th} = 25 \, \mathrm{km \, s^{-1}}$, a probability of more than 5 per cent requires a halo mass of $M_{200} < 1 \times 10^{12} \, M_{\odot}$, rather than $M_{200} < 2 \times 10^{12} \, M_{\odot}$ that is appropriate for $V_{th} = 30 \, \mathrm{km \, s^{-1}}$.

We have also examined the dependence of our results on $N_{200}^{min}(\nu)$, the assumed minimum number of particles needed for convergence (listed in Table 1). This is shown by the red and blue curves in Fig. 5, which correspond to increasing N_{200}^{min} by factors of 4 and 8,
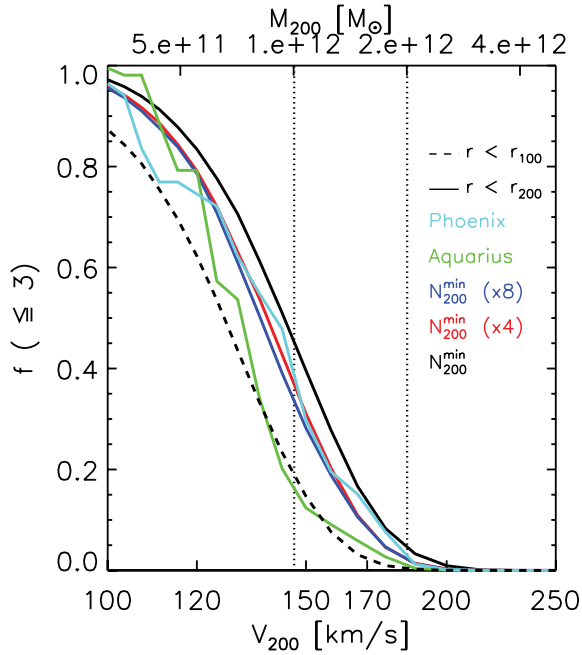
Figure 5. Probability that a halo contains three or fewer subhaloes with $V_{max} > 30$ km s^{-1} as a function of halo mass (top tick marks) or virial velocity (bottom tick marks). The solid black curve corresponds to assuming Poisson statistics and that $N_{sub}(>\nu) = 10.2 \, (\nu/0.15)^{-3.11}$, the average number of subhaloes within the virial radius of well-resolved MS and MS-II haloes with particle numbers exceeding N_{200}^{min} (see Table 1). The sensitivity of the result to the assumed minimum number of particles is shown by the red and blue curves, which correspond to increasing the values of $N_{200}^{min}(\nu)$ by factors of 4 and 8, respectively. Results using only the nine Phoenix or six Aquarius haloes are shown in cyan and green, respectively. Note that because subhaloes are slightly overabundant in Aquarius (see Fig. 4), the probabilities are systematically lower than when considering either Phoenix haloes or the Millennium Simulations. The same is true if subhaloes are identified within a radius larger than the virial radius. The dashed curve shows probabilities when the search radius around each halo is increased by roughly 30 per cent to r_{100}.

respectively, before deriving $\langle N_{sub} \rangle(>\nu)$. Fig. 5 makes it clear that our results are quite insensitive to such changes in N_{200}^{min}.

Since Phoenix haloes have subhalo abundances in good agreement with those in equation (1), our results would not change had we chosen the nine Phoenix haloes to compute $\langle N_{sub} \rangle(>\nu)$ (see the cyan curve in Fig. 5). On the other hand, had we chosen to derive $\langle N_{sub} \rangle(>\nu)$ solely from the six Aquarius haloes, the slight overabundance of subhaloes in these systems would lead to stricter upper limits on the MW halo mass, as shown by the green curve in

Fig. 5. This result, together with the fact that the average Aquarius halo mass (1.42×10^{12} M$_\odot$) is uncomfortably close to the upper limit discussed above, is apparently the reason why Boylan-Kolchin et al. (2011) originally found such a strong discrepancy between the Aquarius simulations and the MW.

Finally, we need to consider the dependence of the number of subhaloes on the maximum radius used to identify substructure. The results discussed above refer to subhaloes identified within the virial radius, r_{200}, which is ~200 kpc for an $M_{200} = 10^{12}$ M$_\odot$ halo. This is smaller than the maximum distance commonly adopted to identify dwarf galaxies as MW satellites; for example, Leo I is at roughly 250 kpc from the centre of the Galaxy. Therefore, it might be argued that subhaloes should be counted within a larger radius in order to make a meaningful comparison. As shown in the bottom panel of Fig. 4, subhaloes are roughly ~50 per cent more abundant within r_{100} than within r_{200}. For an $M_{200} = 10^{12}$ M$_\odot$ halo, $r_{100} \approx 270$ kpc, comparable to the Galactocentric distance of Leo I. In analogy with equation (1), the average number of subhaloes, $N_{sub}(>\nu)$, within r_{100} is well approximated, in the range $0.1 < \nu < 0.5$, by

$$\langle N_{sub} \rangle(>\nu) = 15.03 \, (\nu/0.15)^{-3.06}. \tag{3}$$

The dashed line in Fig. 5 shows that the probability of hosting at most three massive subhaloes drops significantly when the r_{100} radius is used; only about 20 per cent of $M_{200} = 10^{12}$ M$_\odot$ haloes pass the test then. This stricter constraint emphasizes the difficulty of resolving the missing massive satellite problem if the MW mass significantly exceeds 10^{12} M$_\odot$.

4 SUMMARY

We have used the Millennium Simulation series, together with the ultra-high resolution simulations of small halo samples from the Aquarius and Phoenix projects to study the abundance of rare, massive subhaloes in ΛCDM haloes. As in earlier work, we find that the scaled subhalo velocity function (i.e. the number of subhaloes as a function of the ratio between subhalo maximum circular velocity and host halo virial velocity, $\nu = V_{max}/V_{200}$) is independent of halo mass. This implies that we can obtain robust estimates of the statistical distribution of massive subhaloes from large samples of well-resolved haloes selected from the Millennium Simulations.

Our main result is that, in the range $0.1 < \nu < 0.5$, the number of subhaloes within the virial radius, r_{200}, is Poisson distributed around an average given by equation (1). Compared to this average, subhaloes in the Aquarius Project are slightly overabundant but still consistent given the large variance and the small sample of haloes included in that simulation suite. Subhaloes in the cluster-sized Phoenix Project haloes are in excellent agreement with equation (1).

Table 1. $N_{200}^{min}(\nu)$ is the minimum number of particles within the virial radius of a halo needed to achieve convergence in the abundance of subhaloes. N_{haloes} is the number of haloes that satisfy such a condition in the Millennium Simulations. $\langle N_{sub} \rangle$ and $\sigma_{N_{sub}}$ are the average number of subhaloes exceeding ν and its dispersion, respectively.

ν (V_{max}/V_{200})	0.1	0.15	0.2	0.25	0.3	0.35	0.4	0.45	0.5
N_{200}^{min}	1.0×10^6	2.5×10^5	1.2×10^5	7.5×10^4	2.5×10^4	1.8×10^4	1.0×10^4	7.5×10^3	5.0×10^3
N_{haloes}	614	3070	6867	12 138	38 550	54 568	90 200	113 585	151 663
$\langle N_{sub} \rangle$ ($r < r_{200}$)	36.55	10.14	4.20	2.12	1.14	0.71	0.48	0.34	0.25
$\sigma_{N_{sub}}$ ($r < r_{200}$)	8.92	3.87	2.27	1.54	1.10	0.85	0.68	0.57	0.48
$\langle N_{sub} \rangle$ ($r < r_{100}$)	51.91	15.22	6.30	3.11	1.73	1.06	0.69	0.46	0.33
$\sigma_{N_{sub}}$ ($r < r_{100}$)	12.2	5.23	2.99	1.98	1.39	1.08	0.84	0.68	0.58

We have then used this result to compute the probability that a halo of virial velocity V_{200} has a certain number of massive subhaloes with V_{max} exceeding a velocity threshold, V_{th}. Applied to the MW, where observations suggest that no more than three (or at most four) subhaloes with $V_{max} > 30\ km\ s^{-1}$ host luminous satellites, this constraint is found to be effectively translated into a strong upper limit on the MW halo mass. The probability that a halo with $M_{200} \gtrsim 3 \times 10^{12}\ M_\odot$ satisfies this constraint within radius r_{200} is vanishingly small, but it increases rapidly with decreasing virial mass. Roughly 45 per cent of $M_{200} = 10^{12}\ M_\odot$ haloes pass this test, and ~ 90 per cent of all haloes with $M_{200} \sim 5 \times 10^{11}\ M_\odot$ are consistent with the data. These fractions are reduced to ~ 20 and ~ 70 per cent, respectively, if subhaloes are considered within a larger search radius, $r_{100} \sim 1.3\ r_{200}$ (which, for haloes of mass $\sim 10^{12}\ M_\odot$, is close to the Galactocentric distance of Leo I, the most distant bright satellite known in the MW). In this case, the number of subhaloes, $\langle N_{sub}\rangle(>\nu)$, within r_{100} is given by equation (3) and an MW halo mass of $M_{200} = 2 \times 10^{12}\ M_\odot$ is strongly ruled out by the satellite data.

The 'missing massive satellites problem' in the MW halo highlighted by Boylan-Kolchin et al. (2011, 2012) and Parry et al. (2012) may thus be resolved if the mass of the MW halo is $\sim 10^{12}\ M_\odot$ (see also Vera-Ciro et al. 2012). This is well within the range of halo masses allowed by the latest estimates based on either the timing argument (Li & White 2008) or abundance-matching methods (Guo et al. 2010). It is in even better agreement with the lower virial masses reported by estimates based on (i) the radial velocity dispersion of MW satellites and halo stars (Battaglia et al. 2005; Sales et al. 2007), (ii) the escape speed in the solar neighbourhood (Smith et al. 2007) or (iii) the kinematics of halo blue horizontal branch stars (Xue et al. 2008). Invoking an $\sim 10^{12}\ M_\odot$ mass for the MW is a simpler and more straightforward resolution than several alternatives advanced in recent papers, such as considering the baryon adiabatic contraction and feedback (di Cintio et al. 2011), reducing the central density of subhaloes through tidal stripping (Di Cintio et al. 2012; Vera-Ciro et al. 2012), or positing radical revisions to the nature of dark matter (Lovell et al. 2012; Vogelsberger, Zavala & Loeb 2012).

We conclude that there is no compelling requirement to revise the ΛCDM paradigm based on the abundance of massive subhaloes in the MW. There are still, however, some uncomfortable corollaries to this solution. One is that a $10^{12}\ M_\odot$ halo has a virial velocity of only $\sim 150\ km\ s^{-1}$, well below the rotation speed of the MW disc, usually assumed to be $V_{rot} = 220\ km\ s^{-1}$, or even higher (Reid et al. 2009). This seems at odds with results from some semi-analytic models of galaxy formation that attempt simultaneously to match the Tully–Fisher relation and the galaxy stellar mass function; agreement with observation seems to require $V_{rot} \approx V_{200}$ (see e.g. Cole et al. 2000; Croton et al. 2006).

A further worry is that an $M_{200} = 10^{12}\ M_\odot$ halo might not be massive enough to host satellites as massive as the Magellanic Clouds. Assuming that V_{max} for the Large Magellanic Cloud (LMC) and Small Magellanic Cloud (SMC) can be identified with the rotation speed of their H I discs, 60 and 50 $km\ s^{-1}$, respectively (Kim et al. 1998; Stanimirović, Staveley-Smith & Jones 2004), we find, using the data in Table 1, that only ~ 62 per cent of $V_{200} = 150\ km\ s^{-1}$ haloes would be expected not to host an LMC-like system. The probability of hosting two (or more) subhaloes more massive than the SMC is of the order of 20 per cent. None of these probabilities seem unlikely enough to cause worry.

Although our results may explain why few massive subhaloes might be expected in the MW halo, this explanation still assigns

MW satellites to very low mass haloes, i.e. those with $V_{max} < 30\ km\ s^{-1}$. These haloes have masses below $10^{10}\ M_\odot$, the mass scale below which semi-analytic models predict that galaxy formation efficiency should become exceedingly small (Guo et al. 2010). Given the large number of low-mass haloes expected in a ΛCDM universe, populating even a small fraction of $V_{max} < 30\ km\ s^{-1}$ systems with galaxies as bright as Fornax might lead to substantially overpredicting the number of dwarfs in the local Universe (see e.g. Ferrero et al. 2011). Without a full accounting of how dwarf galaxies form in low-mass haloes, concerns about the viability of ΛCDM on small scales will be hard to dispel.

REFERENCES

Battaglia G. et al., 2005, MNRAS, 364, 433
Benson A. J., Lacey C. G., Baugh C. M., Cole S., Frenk C. S., 2002, MNRAS, 333, 156
Boylan-Kolchin M., Springel V., White S. D. M., Jenkins A., Lemson G., 2009, MNRAS, 398, 1150
Boylan-Kolchin M., Springel V., White S. D. M., Jenkins A., 2010, MNRAS, 406, 896
Boylan-Kolchin M., Bullock J. S., Kaplinghat M., 2011, MNRAS, 415, L40
Boylan-Kolchin M., Bullock J. S., Kaplinghat M., 2012, MNRAS, 422, 1203
Bullock J. S., Kravtsov A. V., Weinberg D. H., 2000, ApJ, 539, 517
Cole S., Lacey C. G., Baugh C. M., Frenk C. S., 2000, MNRAS, 319, 168
Cooper A. P. et al., 2010, MNRAS, 406, 744
Croton D. J. et al., 2006, MNRAS, 365, 11
di Cintio A., Knebe A., Libeskind N. I., Yepes G., Gottlöber S., Hoffman Y., 2011, MNRAS, 417, L74
Di Cintio A., Knebe A., Libeskind N. I., Brook C., Yepes G., Gottloeber S., Hoffman Y., 2012, MNRAS, 417, 74
Ferrero I., Abadi M. G., Navarro J. F., Sales L. V., Gurovich S., 2011, preprint (arXiv:e-prints)
Font A. S. et al., 2011, MNRAS, 417, 1260
Gao L., Navarro J. F., Frenk C. S., Jenkins A., Springel V., White S. D. M., 2012, preprint (arXiv:e-prints)
Guo Q., White S., Li C., Boylan-Kolchin M., 2010, MNRAS, 404, 1111
Guo Q. et al., 2011, MNRAS, 413, 101
Kauffmann G., White S. D. M., Guiderdoni B., 1993, MNRAS, 264, 201
Kim S., Staveley-Smith L., Dopita M. A., Freeman K. C., Sault R. J., Kesteven M. J., McConnell D., 1998, ApJ, 503, 674

Komatsu E. et al., 2011, ApJS, 192, 18

Kravtsov A. V., Berlind A. A., Wechsler R. H., Klypin A. A., Gottlöber S., Allgood B., Primack J. R., 2004, ApJ, 609, 35

Li Y.-S., White S. D. M., 2008, MNRAS, 384, 1459

Li Y.-S., De Lucia G., Helmi A., 2010, MNRAS, 401, 2036

Łokas E. L., 2009, MNRAS, 394, L102

Lovell M. R. et al., 2012, MNRAS, 420, 2318

Macciò A. V., Kang X., Fontanot F., Somerville R. S., Koposov S., Monaco P., 2010, MNRAS, 402, 1995

Moore B., Ghigna S., Governato F., Lake G., Quinn T., Stadel J., Tozzi P., 1999, ApJ, 524, L19

Parry O. H., Eke V. R., Frenk C. S., Okamoto T., 2012, MNRAS, 419, 3304

Peñarrubia J., McConnachie A. W., Navarro J. F., 2008a, ApJ, 672, 904

Peñarrubia J., Navarro J. F., McConnachie A. W., 2008b, ApJ, 673, 226

Reid M. J. et al., 2009, ApJ, 700, 137

Sales L. V., Navarro J. F., Abadi M. G., Steinmetz M., 2007, MNRAS, 379, 1464

Smith M. C. et al., 2007, MNRAS, 379, 755

Somerville R. S., 2002, ApJ, 572, L23

Springel V., Yoshida N., White S. D. M., 2001, New Astron., 6, 79

Springel V. et al., 2005, Nat, 435, 629

Springel V. et al., 2008, MNRAS, 391, 1685

Stanimirović S., Staveley-Smith L., Jones P. A., 2004, ApJ, 604, 176

Strigari L. E., Bullock J. S., Kaplinghat M., Simon J. D., Geha M., Willman B., Walker M. G., 2008, Nat, 454, 1096

Strigari L. E., Frenk C. S., White S. D. M., 2010, MNRAS, 408, 2364

Vera-Ciro C. A., Helmi A., Starkenburg E., Breddels M. A., 2012, preprint (arXiv:e-prints)

Vogelsberger M., Zavala J., Loeb A., 2012, preprint (arXiv:e-prints)

Walker M. G., Mateo M., Olszewski E. W., Peñarrubia J., Wyn Evans N., Gilmore G., 2009, ApJ, 704, 1274

Weinberg D. H., Colombi S., Davé R., Katz N., 2008, ApJ, 678, 6

White S. D. M., Frenk C. S., 1991, ApJ, 379, 52

Wolf J., Martinez G. D., Bullock J. S., Kaplinghat M., Geha M., Muñoz R. R., Simon J. D., Avedo F. F., 2010, MNRAS, 406, 1220

Xue X. X. et al., 2008, ApJ, 684, 1143

Zheng Z. et al., 2005, ApJ, 633, 791

This paper has been typeset from a TEX/LATEX file prepared by the author.